Polymer Chemistry

PGMA-based supramolecular hyperbranched polycations for gene delivery†

Miao Qi,‡[a] Shun Duan,‡[b,c] Bingran Yu,[c] Hao Yao,[a] Wei Tian*[a] and Fu-Jian Xu*[b,c]

Supramolecular chemistry has been widely applied in biomedical fields. It was reported that the topological structure has effects on the performance of gene delivery systems. Supramolecular polymer-like gene carriers with hyperbranched topological structures have still not been reported. In this work, a series of ethanolamine-functionalized polyglycidyl methacrylate (PGMA)-armed AB$_2$ type macromonomers were synthesized based on atom transfer radical polymerization. The AB$_2$ type macromonomers can self-assemble into supramolecular hyperbranched polymers by the host–guest interaction between adamantane and β-cyclodextrin. The biophysical properties of self-assembled and dissembled supramolecular hyperbranched polycations were evaluated in detail. The self-assembled supramolecular polycations with hyperbranched structures possessed higher pDNA condensation ability and much better gene transfection performances than the dissembled AB$_2$ type counterparts. The present work would provide a new venue for designing advanced high-performance supramolecular hyperbranched nucleic acid-delivery systems.

Introduction

Gene therapy is a promising strategy for various serious diseases, such as cancers, cardiovascular diseases, genetic disorders, and acquired immune deficiency syndrome.[1–3] In the process of DNA or RNA delivery into cells, nucleic acid carriers play an essential role. Although having high transfection efficiency, viral carriers demonstrate many safety problems including induction of immunological response and potential integration of host genomes.[4] Compared with viral carriers, non-viral carriers, mainly consisting of polycations, have lower immunogenicity and higher tenability of performance and function.[5] Therefore, the study of gene delivery systems based on polycations is becoming a hot spot issue. In the past few years, a wide range of polycations have been investigated as gene carriers, including polyethylenimine (PEI), poly(amino acids), and poly((2-dimethyl amino)ethyl methacrylate).[6–8]

[a]*The Key Laboratory of Space Applied Physics and Chemistry, Ministry of Education and Shaanxi Key Laboratory of Macromolecular Science and Technology, School of Science, Northwestern Polytechnical University, Xi'an, 710072, P. R. China. E-mail: happytw_3000@nwpu.edu.cn*
[b]*Key Laboratory of Carbon Fiber and Functional Polymers (Beijing University of Chemical Technology), Ministry of Education, Beijing 100029, China. E-mail: xufj@mail.buct.edu.cn*
[c]*Beijing Laboratory of Biomedical Materials, Beijing University of Chemical Technology, Beijing 100029, China*
†Electronic supplementary information (ESI) available. See DOI: 10.1039/c6py00759g
‡The authors contributed equally to this work.

However, the polycations still have some shortcomings on their safety and performance, such as cytotoxicity and low transfection efficiency.

Recently, many studies have been conducted to improve the transfection performances of polycations. A kind of versatile polymer, polyglycidyl methacrylate (PGMA), has drawn much attention of researchers on biomedical materials.[9] On this basis, a promising gene delivery system based on the ethanolamine (EA) functionalized PGMA (denoted by BUCT-PGEA) was reported.[10] PGMA-based polycations with different molecular structures were developed, such as linear, comb-like, and star-like structures.[11–13] It was reported that the topological structure also has effects on the performances of gene delivery systems. Hyperbranched structures could facilitate the formation of a polycation/DNA complex and benefit the performance of gene/drug delivery.[14–17] However, the cytotoxicity of gene carrier would be increased with increasing molecular weights.[18] To solve this problem, the supramolecular structure has drawn great attention in biomedical material fields.[19] Particularly, supramolecular polymers as a potential strategy could be considered because of their non-covalent structure, specific physicochemical properties and designable functions.[20]

A supramolecular polymer is a complex molecular structure formed by non-covalent bonds, such as electrostatic force, hydrogen bonding, π–π stacking and hydrophobic/hydrophilic interactions.[21–25] A supramolecular polymer has many unique thermodynamic properties which endow it with a capacity of assembly at higher order structures.[26] Therefore, the study of

supramolecular polymers in drug delivery fields has drawn great attention in recent years.[27,28] The host molecules of host–guest recognition include cucurbiturils (CBs),[29] cyclodextrins (CDs),[30] crown ethers,[31] calixarenes,[32] and pillararenes.[33] Among these host molecules, CDs exhibited good performance in gene/drug delivery systems.[34–36] Various supramolecular polymers were investigated,[37–40] and some of them were applied in biomedical fields.[37]

Supramolecular polycations with a linear structure had been investigated, and their transfection efficiencies were not higher than gold-standard branched PEI (25 kDa).[41] However, the study on supramolecular polymer-like gene carriers with hyperbranched topological structures has still not been reported. Herein one kind of PGMA-based supramolecular hyperbranched polycation was proposed for efficient gene delivery. A series of AB$_2$ macromonomers (Ad-(CD-PGEA)$_2$, ACP) with one adamantane (Ad) group and two CD-PGEA arms with different lengths were first synthesized (Scheme 1). ACPs could self-assemble into supramolecular hyperbranched polymers in aqueous solution based on the host–guest interactions between Ad and β-CD units. The transfection performances of the self-assembled and dissembled supramolecular hyperbranched polycations (denoted as S-ACP and D-ACP, respectively) were investigated in detail. The present work may provide a new concept to develop a kind of highly efficient supramolecular gene delivery system.
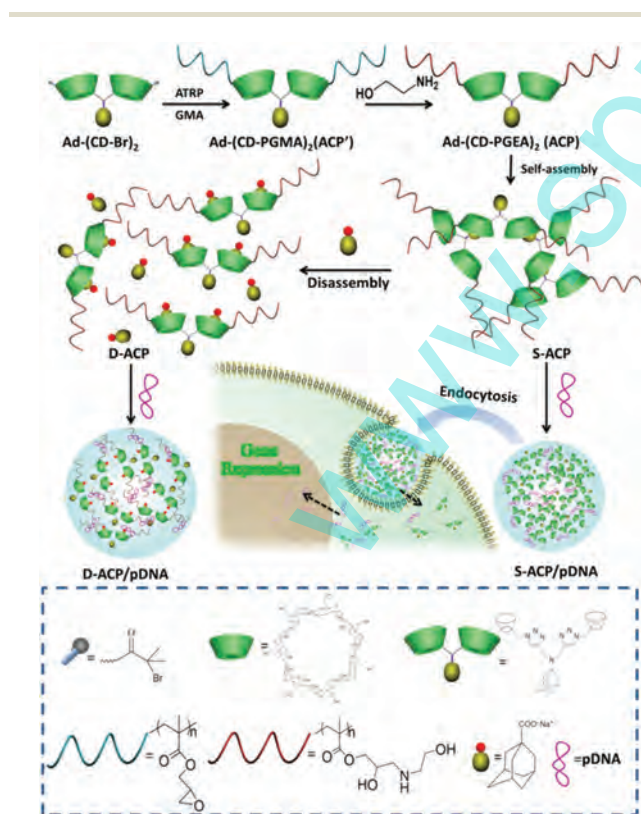
Scheme 1 Schematic diagram illustrating the preparation of PGMA-based supramolecular hyperbranched polycations and their resultant pDNA delivery process.

Experimental

Materials

Ad-CD$_2$ was synthesized according to the method reported in our previous work.[38] α-Bromoisobutyryl bromide (98%), trimethylamine (AR, 99.0%), 4-dimethylaminopyridine (99%) and ethanolamine (AR, 99.0%) were purchased from Sinopharm Chemical Reagent Co., Ltd, China. N,N,N′,N″,N″-Pentamethyldiethylenetriamine (PMDETA), copper(I) bromide (CuBr, 98%) and glycidyl methacrylate (GMA, 97%) were purchased from Sigma-Aldrich Chemical Co.

Synthesis of Ad-(CD-Br)$_2$

Ad-CD$_2$ (700 mg, 0.275 mmol), triethylamine (TEA) (111.1 mg, 1.1 mmol) and 4-dimethylaminopyridine (33.55 mg, 0.275 mmol) were dissolved in 3 mL of anhydrous N,N-Dimethylformamide with stirring and then the mixture was cooled to 0 °C. Subsequently, a solution of α-bromoisobutyryl bromide (253 mg, 1.1 mmol) in anhydrous N,N-Dimethylformamide (3 mL) was added dropwise to the Ad-CD$_2$ solution for a period of 20 min at 0 °C. After the addition, the reaction temperature was maintained at 0 °C for another 1 h and then allowed to rise slowly to room temperature (r.t.), after which the reaction was allowed to continue for 24 h. The final reaction mixture was precipitated with 300 mL of diethyl ether. The resulting white powder was collected by filtration, and washed with acetone (2 × 30 mL), producing Ad-(CD-Br)$_2$. In the purification process, the crude product was suspended in 15 mL of deionized water, and the mixture was stirred at r.t. overnight. The purified product was precipitated with 300 mL of diethyl ether, collected by filtration, washed with acetone (2 × 30 mL), and dried under vacuum. Yield 6.30 g (76.2%, based on an average substitution degree of 2). FTIR: 1736 cm^{-1} (–COO–), 3350 cm^{-1} (–OH), 663 cm^{-1} (C–Br); ^{1}H NMR (400 MHz, DMSO-d_6, room temperature, TMS): δ_H (ppm) = 3.12–3.42 (2,4-H, 14H), 3.49–3.82 (3,5,6-H, 28H), 4.40–4.58 (6-OH, 5H), 4.75–4.92 (1-H, 7H), 5.52–5.92 (2,3-OH, 14H), 7.89 (protons from triazole, 2H), 2.09 (–CH–, 3H), 1.91 (–CH$_3$, 12H), 1.77 (–C–CH$_2$–, 6H), 1.59 (–CH–CH$_2$–, 6H); ^{13}C NMR (400 MHz, DMSO-d_6, room temperature, TMS): δ_C (ppm) = 171.12 (–COO–), 146.79, 125.72 (carbons from triazole), 102.21 (C-1), 81.88 (C-4), 72.52 (C-2,3,5), 60.26 (C-6), 57.60 (–COC(CH$_3$)$_2$Br), 55.17 (–NCH$_2$C), 36.70 (–NCH$_2$CH–, –CHCH$_2$CH), 30.60 (–C(Br)CH$_3$), 29.25 (–CH$_2$CHCH$_2$–). MALDI-TOF-MS (DMF, m/z): calcd for C$_{108}$H$_{169}$O$_{70}$N$_7$Br$_2$: 2845.3; found for [M + Na]$^+$: 2869.0.

Synthesis of Ad-(CD-PGMA)$_2$

Ad-(CD-PGMA)$_2$ was synthesized by the atom transfer radical polymerization (ATRP) of GMA using Ad-(CD-Br)$_2$ as the macroinitiator. In a typical example, GMA (213.3 mg, 1.5 mmol), PMDETA (26 mg, 0.15 mmol), Ad-(CD-Br)$_2$ (142.25 mg, 0.05 mmol), and 1 mL DMF were charged into a reaction flask. The flask was capped with a rubber plug and purged with pure nitrogen for 30 min. CuBr (14.4 mg, 0.1 mmol) was then introduced under the protection of N$_2$ flow to start the polymerization at 60 °C under a nitrogen atmosphere. After 6 h, the

Table 1 Molecular weights and molecular weight distributions of ACP′ 1–3

Sample	$DP_{PGMA,NMR}$ [a]	$M_{n,NMR}$ [a]	$M_{w,SEC/MALLS}$ [b]	$M_{n,SEC/MALLS}$ [b]	M_{w}/M_{n} [b]
ACP′1	16	5100	6500	5200	1.25
ACP′2	26	6500	7600	6700	1.13
ACP′3	33	7500	10 700	8900	1.20

[a] Degree of polymerization (DP) of every PGMA arm determined by the integration of methylene of epoxy groups to protons of β-CD in the C-1 position. Thus, the molecular weights of ACP′1–3 can be calculated by the following formula.

$$M_{nACP's} = M_{Ad-(CD-Br)_2} + M_{GMA} \times \text{Monomer repeat units};$$
$$M_{Ad-(CD-Br)_2} = 2845 \text{ g mol}^{-1}, M_{GMA} = 142.2 \text{ g mol}^{-1}$$

[b] Molecular weights and molecular weight distributions determined by SEC/MALLS, and the average dn/dc value was 0.065.

reaction mixture was diluted with DMF and passed through neutral alumina to remove the copper catalyst. The polymer was obtained from the resulting reaction mixture by concentrating DMF to 1 mL. Such a mixture was placed in a dialysis membrane (MWCO, 3500 Da) and then purified by dialyzing in DMF for 2 days and in deionized water for another 3 days to remove the unreacted monomers and macroinitiators. After removal of water by freeze drying, a white powder was obtained (183 mg, yield: 51%). By changing the ATRP polymerization time, a series of Ad-(CD-PGMA)$_2$ samples denoted as ACP′1, ACP′2, and ACP′3 were obtained. FTIR of ACP′1: 3350 cm^{-1} (–OH), 865 cm^{-1} (–CH$_2$(O)CH$_2$–), 659 cm^{-1} (C–Br); ^{1}H NMR of ACP′1 (400 MHz, DMSO-d_6, room temperature, TMS): δ (ppm) = 3.12–3.42 (2,4-H, 14H), 3.49–3.82 (3,5,6-H, 28H), 4.40–4.58 (6-OH, 5H), 4.75–4.92 (H-1, 7H), 5.52–5.92 (2,3-OH, 14H), 1.91 (–CH$_3$, 12H), 1.5–2.1 (Ad, 15H), 4.19–4.24, 3.70–3.89 (protons from methylene adjacent to the epoxy group, 2H), 3.11–3.26 (proton from methine in the epoxy group, 1H), 2.57–2.91 (protons from methylene in the epoxy group, 2H), 1.82 (–CH$_2$Br, 2H), 0.81 (–CCH$_3$, 3H); ^{13}C NMR (400 MHz, DMSO-d_6, room temperature, TMS): δ$_C$ (ppm) = 177.14 (–COO–), 65.84 (carbons adjacent to the epoxy group), 53.44 (–CCH$_3$), 49.01 (carbon from methine in the epoxy group), 44.30 (carbons from methylene in the epoxy group), 18.65 (–CH$_2$Br), 16.67 (–CCH$_3$). Molecular weights and their distributions of ACP′1–3 are shown in Table 1.

Synthesis of Ad-(CD-PGEA)$_2$

Ad-(CD-PGEA)$_2$ was prepared by reacting Ad-(CD-PGMA)$_2$ with excess ethanolamine (EA). Ad-(CD-PGMA)$_2$ (0.2 g) was dissolved in DMSO (5 mL). EA (2.5 mL) and TEA (1 mL) were then added. The reaction mixture was stirred at room temperature for 5 days to produce Ad-(CD-PGEA)$_2$. The final reaction mixture was precipitated with excess diethyl ether. The crude produce was re-dissolved in 10 mL of deionized water and dialyzed against deionized water with the dialysis membrane (MWCO, 3500 Da) at room temperature for 24 h. A white powder was obtained (140 mg, yield: 51%). A series of Ad-(CD-PGEA)$_2$ samples denoted as ACP1, ACP2, and ACP3 were

obtained. FTIR of ACP1: 1724 cm^{-1} (–NH–), 1154 cm^{-1} (–C–N–); ^{1}H NMR of ACP1 (400 MHz, DMSO-d_6, room temperature, TMS): δ (ppm) = 3.12–3.42 (2,4-H, 14H), 3.49–3.82 (3,5,6-H, 28H), 4.40–4.58 (6-OH, 5H), 4.75–4.92 (1-H, 7H), 5.52–5.92 (2,3-OH, 14H), 1.91 (–CH$_3$,12H), 1.5–2.1 (Ad, 15H), 3.71–3.98 (–OCH$_2$CHOH–), 3.12–3.59 (–CH$_2$CH(OH)CH$_2$– and –CH$_2$CH$_2$OH), 2.52–2.78 (–CH(OH)CH$_2$NH– and –NHCH$_2$CH$_2$OH); ^{13}C NMR (400 MHz, DMSO-d_6, room temperature, TMS): δ$_C$ (ppm) = 177.37 (–COO–), 67.46 (–OCH$_2$CH(OH)–), 60.61 (–CH$_2$CH$_2$OH), 51.77 (–CH(OH)CH$_2$(NH)–, –NHCH$_2$CH$_2$OH), 44.61 (–CH$_2$CH(OH)CH$_2$).

Formation and dissociation of S-ACPs

The construction of S-ACPs was based on the host–guest interaction between β-CD and Ad species. In a typical experiment, ACP1 (2.65 mg) was dissolved in 1.0 mL deionized water and stirred overnight to obtain S-ACP1. S-ACP2 (2.46 mg mL^{-1}) and S-ACP3 (2.38 mg mL^{-1}) were obtained by a similar method. In all the solutions of ACPs, the concentration of the nitrogen element was 10 nmol mL^{-1}. To obtain D-ACPs, an appropriate amount of Ad-Na (e.g. 1.88 mg, 8.7×10^{-3} mM, the molar ratio of Ad-Na to CD in ACP1 = 10 : 1) was added to the S-ACP solutions to achieve morphology transitions of supramolecular hyperbranched polycations in water.

Characterization of S-ACP

2D ^{1}H NMR NOESY spectra were recorded on a Bruker-Avance III NMR spectrometer (400 MHz) with D$_2$O as the solvent. Transmission electron microscopy (TEM) observations were conducted on a Hitachi H-7650 electron microscope at an acceleration voltage of 75 kV. Samples were prepared by dropping 10 μL of polymer solutions on copper grids with staining for 4 minutes, which was then treated with cold liquid nitrogen quenching and vacuum freeze-drying. The morphology was also visualized using atomic force microscopy (AFM) with the tapping mode and a Nanowizard II controller (Benyuan, CSPM 5500, China). Samples were prepared by dropping 20 μL of polymer solutions onto freshly mica plates and then vacuum dried at 25 °C.

Preparation and characterization of S-ACP/pDNA complexes

S-ACP solutions were prepared at a nitrogen concentration of 10 nmol mL^{-1} in distilled water, and the pDNA concentration was 0.1 mg mL^{-1} in Tris-EDTA buffer (pH 7.4). The ratio of S-ACP to pDNA was expressed as the molar ratio of nitrogen (N) in polymer to phosphorus (P) in pDNA. The S-ACP/pDNA complexes were prepared by mixing S-ACP and pDNA solutions at different N/P ratios, followed by vortexing and incubation for 30 min at room temperature. The pDNA condensation ability of S-ACP was evaluated by agarose gel electrophoresis as described in our earlier work.[43] The sizes and zeta-potentials of the complexes were measured by using a Zetasizer Nano ZS (Malvern Instruments, UK). The morphologies of the S-ACP/pDNA complexes were observed by AFM (Bruker, USA), and the images were analyzed by using Nanoscope software.

Cell viability

CCK-8 assay was performed to study the cytotoxicity of S-ACP and D-ACP in C6 cell lines. C6 cells were cultured in modified Dulbecco's Eagle medium (DMEM, Hyclone, USA) supplemented with 10% fetal bovine serum (PAA, Germany), 100 IU per mL penicillin (Sigma, USA) and 100 mg per mL streptomycin (Sigma, USA) in an incubator (Sanyo, Japan) with 5% CO_2 at 37 °C and saturated humidity. When the cells had grown to 80% confluence, they were digested and seeded into 96-well plates at a density of 10^4 cells per well with 100 μL culture media. After 24 h culture, the culture media were replaced with 100 μL culture media containing 10 μL of complex solution at various N/P ratios and cultured for 4 h, and then the media were replaced with fresh media and cultured for another 20 h. The cell viability was measured by the CCK-8 assay as described in our previous work.[44] The relative cell viability was calculated by using the equation $[A]_{sample}/[A]_{control} \times 100\%$, where the absorbance ([A]) of each well was measured in a microplate reader (Bio-rad 680, USA) at a wavelength of 450 nm.

Transfection assay

The transfection efficiencies of S-ACPs were evaluated using a pRL-CMV plasmid as the reporter gene in C6 cell lines. The C6 cells were seeded into 24-well plates at a density of 5×10^4 cells per well with 500 μL culture media and cultured for 24 h. In each well, 20 μL of S-ACP/pDNA complexes at the N/P ratios from 5 to 30 containing 1 μg of pDNA was added. The cells were incubated for 4 h to facilitate gene transfection. Then, the culture media were replaced with 500 μL fresh media and cultured for another 20 h. The expression of the luciferase gene was measured using a commercial kit (Promega Co., CergyPontoise, France). Before the gene expression assay, the cells were rinsed with phosphate buffer saline (PBS, Hyclone, USA) and lysed with 100 μL lysis buffer solution (Promega Co., CergyPontoise, France). The expressed luciferase was quantified by using a luminometer (Berthold Lumat LB 9507, Berthold Technologies GmbH. KG, Bad Wildbad, Germany) and the protein concentration of the lysis was measured using a bicinchoninic acid assay (Biorad Lab, Hercules, CA). The efficiency of luciferase gene expression was presented as relative light units (RLUs) per milligram of protein. In order to visualize the gene transfection performance of S-ACP at its optimal N/P ratio, the enhanced green fluorescent protein (EGFP) plasmid was taken as another reporter gene. The procedures were the same as described above and the images were observed by using a confocal laser scanning microscope (SP8, Leica, Germany). The percentage of EGFP-positive cells was measured by flow cytometry (Beckman Coulter, Pasadena, CA).

Statistical analysis

The experiments were performed in triplicate. The data were represented as mean ± standard deviation for $n = 3$. Statistics analysis was made based on the t-test, and the difference between groups was considered as significant for $p \leq 0.05$.

Results and discussion

Construction and characterization of S-ACP

As shown in Scheme 1, a series of S-ACPs were constructed based on the host–guest interactions between β-CD and Ad by directly dissolving the corresponding Ad-(CD-PGEA)$_2$ (ACP) counterparts in water. For the preparation of ACP, the starting Ad-(CD-PGMA)$_2$ (ACP′) was first synthesized via ATRP using an Ad-(CD-Br)$_2$ macroinitiator. The molecular weights of ACP′1, ACP′2, and ACP′3 were determined by ^{1}H NMR and SEC/MALLS, indicating that the molecular weights increased with the increase of polymerization time, as shown in Table 1. Then, ACP′1–3 were functionalized with excess EA by ring-opening addition to produce ACP1–3 with abundant secondary amine groups. The detailed synthesis and chemical characterization of Ad-(CD-Br)$_2$, ACP′1–3, and ACP1–3 are shown in the ESI (Scheme S1 and Fig. S1–S8†). The 2D ^{1}H NMR NOESY spectra of the typical ACP2 solutions showed that the signals of a, b, and c protons in Ad were well correlated with the signals of the inner protons 3-H and 5-H in β-CD (Fig. 1A). This result indicated that the signals corresponding to Ad were broadened and shifted downfield when the solvent was changed from DMSO to D$_2$O, which further proved the host–guest interaction (Fig. 1B).[37] These observations indicate the occurrence of the complexation between the β-CD and Ad moieties. It was also observed that the ^{1}H NMR spectra signals from the above results indicated that S-ACP was successfully constructed through the host–guest inclusions between the β-CD and Ad moieties of ACP.

The morphologies of S-ACPs in aqueous solution were visualized through TEM and AFM. A branched morphology was gradually formed with the increase of the molecular weight of S-ACP as shown in Fig. 2. Similar results were also reported by Zhou and Zhu et al.[45] Furthermore, S-ACPs could be further
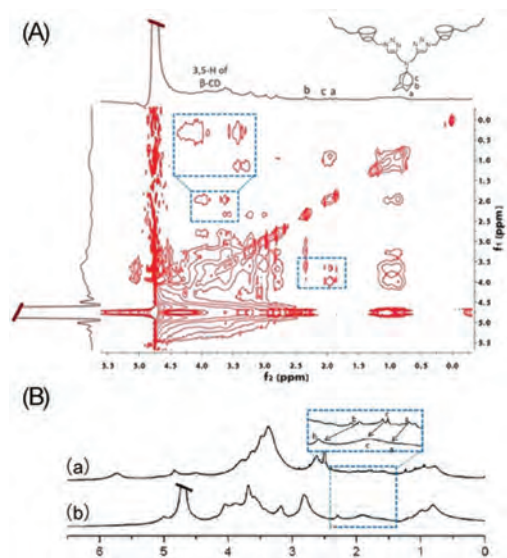
Fig. 1 (A) 2D ^{1}H NMR NOESY spectra of ACP2 in D$_2$O and (B) ^{1}H NMR spectra of ACP2 in (a) DMSO-d_6 and (b) D$_2$O.
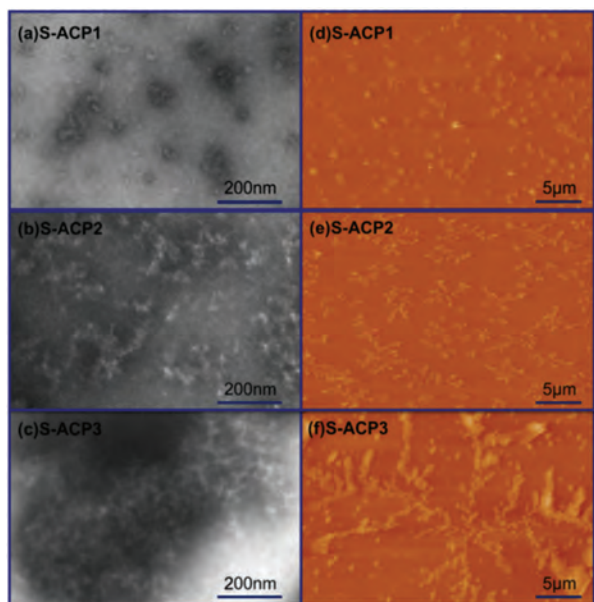
Fig. 2 Typical TEM (a–c) and AFM (d–f) images of S-ACPs in aqueous solutions. For TEM, all samples were stained with phosphotungstic acid.

dissociated in the presence of sodium adamantate (Ad-Na) based on the competitive inclusion interaction between β-CD and two guests according to our recent work.[42] The dissociated samples were named D-ACPs. From the TEM image of D-ACP2 (Fig. S9, ESI†), the spherical aggregations with an average size of 45 nm were formed instead of branched morphologies, indicating the occurrence of dissociation in S-ACPs.

Biophysical characterization of S-ACP/pDNA complexes

Efficient gene carriers should condense pDNA into nanoparticles in order to facilitate cellular uptake. The pDNA-condensing capability of S-ACP was analysed by the electrophoretic mobility of S-ACP/pDNA complexes in the agarose gel at various N/P ratios (Fig. 3). At the N/P ratio of 1.5,
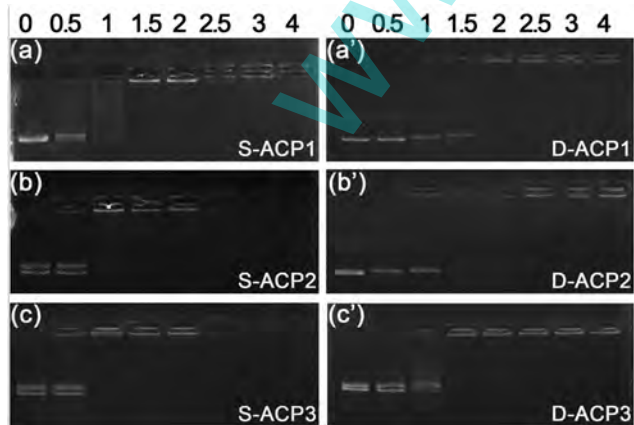
the pDNA didn't migrate under the electronic field, which indicated that S-ACP1 with the lowest molecular weight could condense pDNA completely at this N/P ratio. With the increasing molecular weight, the condensing capabilities of S-ACPs also increased. For S-ACP2 and S-ACP3, the pDNA molecules stayed in the sample wells, which meant that the migration of pDNA was inhibited at the N/P ratio of 1. However, after the disassembly of S-ACPs, the condensation ability decreased accordingly. Compared with the corresponding S-ACP counterparts, all D-ACPs showed lower condensation ability, which demonstrated the effects of the supramolecular structure on the condensation ability.

The particle sizes and zeta potentials of S-ACP/pDNA complexes had great effects on cellular uptake. The particle sizes of S-ACP/pDNA complexes decreased with increasing N/P ratios and molecular weights (Fig. 4a). The particle sizes ranged from 150 to 250 nm when the N/P ratios were higher than 20, which was suitable for cell uptake.[46] The particle sizes of D-ACP/pDNA complexes were much larger than their corresponding counterparts at the same N/P ratio, indicating that the S-ACP had better ability to condense pDNA into nanoparticles than D-ACP. Zeta potential is another essential property to affect cellular uptake. Positive surface charge could facilitate nanoparticles to be attracted onto the negatively-charged cell membrane, thereby enhancing the following endocytosis. The zeta potentials of S-ACP increased with the N/P ratio and molecular weights. Moreover, similar to the results of particle size measurements, the supramolecular structure also had significant effects on the zeta potential (Fig. 4b). At the same N/P ratio, S-ACPs had higher zeta potentials than those of the corresponding D-ACP counterparts, which also meant that S-ACPs had better condensation ability of pDNA.

Fig. 3 Electrophoretic mobility of pDNA in the complexes of S-ACP and D-ACP.
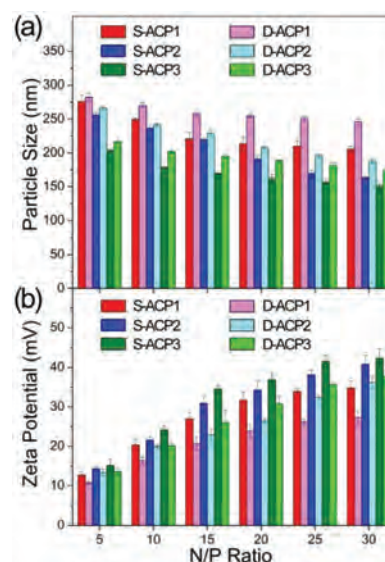
Fig. 4 Particle sizes (a) and zeta-potentials (b) of S-ACP/pDNA and D-ACP/pDNA complexes at various N/P ratios.
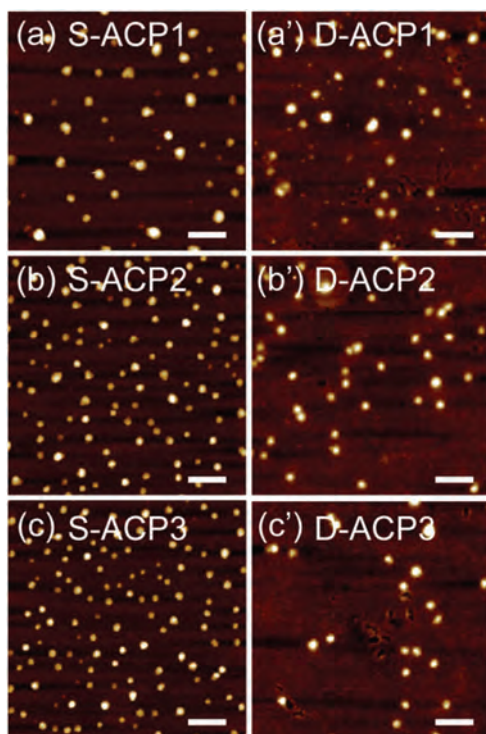
Fig. 5 AFM images of S-ACP/pDNA and D-ACP/pDNA complexes at the N/P ratio of 25 (scale bar = 1 μm).

Fig. 6 (a) Cell viability of the C6 cells treated by S-ACP/pDNA and D-ACP/pDNA complexes at various N/P ratios and (b) *in vitro* luciferase gene transfection efficiency of S-ACP/pDNA and D-ACP/pDNA complexes in comparison with branched PEI (25 kDa) at its optimal N/P ratio of 10.

In addition, the morphologies of the S-ACP/pDNA were imaged by AFM. As shown in Fig. 5, at a typical N/P ratio of 25, S-ACP and D-ACP could condense pDNA into nanoparticles, and the sizes of S-ACP/pDNA complexes were smaller than the D-ACP counterparts, which was consistent with their pDNA condensation abilities. Compared with D-ACP, the better DNA condensation abilities of S-ACP were probably due to the high molecular weight of the supramolecular polymers.

Cytotoxicity assay

The most important application of gene carriers is tumour therapy. To investigate the biological properties of S-ACP and D-ACP, the C6 cell line, a commonly used glioma cell line, was selected for the following biological experiments. A good gene delivery system should have low cytotoxicity. As shown in Fig. 6a, the cytotoxicity of S-ACP and D-ACP increased with the molecular weight and N/P ratio. However, in comparison with gold-standard branched PEI (25 kDa), both S-ACP and D-ACP exhibited significantly lower cytotoxicity because of the low cytotoxicity of aminated PGMA.[9–12] The nonionic hydrophilic hydroxyl groups of aminated PGMA could shield parts of excess positive charge and reduce the toxicity of complexes. Even at the high N/P ratio of 30, the S-ACP still showed more than 50% cell viability while PEI exhibited lower than 20% viability. The slight difference in viabilities between S-ACP and D-ACP at the same N/P ratio was mainly due to the toxicity of Ad-Na (Fig. S10†). The above results indicated that S-ACP had low cytotoxicity.

In vitro gene transfection

Transfection efficiency was assayed using luciferase and EGFP as reporter genes. Fig. 6b shows that the transfection efficiencies mediated by S-ACP and D-ACP increased with the molecular weight at the same N/P ratio. The transfection efficiencies firstly increased with the N/P ratio and then slightly decreased at higher N/P ratios. The toxicity of cationic polymers had more negative effects on cell viability at higher N/P ratios, leading to the reduction of transfection efficiency. At the optimal N/P ratio of 25, the transfection efficiencies of all S-ACPs were higher than the gold-standard of a gene delivery carrier, branched PEI (M_w = 25 kDa). In comparison with S-ACP, the corresponding D-ACP had relatively low transfection efficiencies at their optimal N/P ratios, which was consistent with their pDNA condensation abilities (Fig. 3 and 4). To visualize the gene transfection performance and further demonstrate the effects of supramolecular structures on gene delivery, pEGFP was taken as a reporter gene. As shown in Fig. 7, the EGFP-positive cells (36%) of the S-ACP3 group were more than those (22%) of the D-ACP3 group, which was consistent with the luciferase expression results shown in Fig. 6b. The above results confirmed that the supramolecular
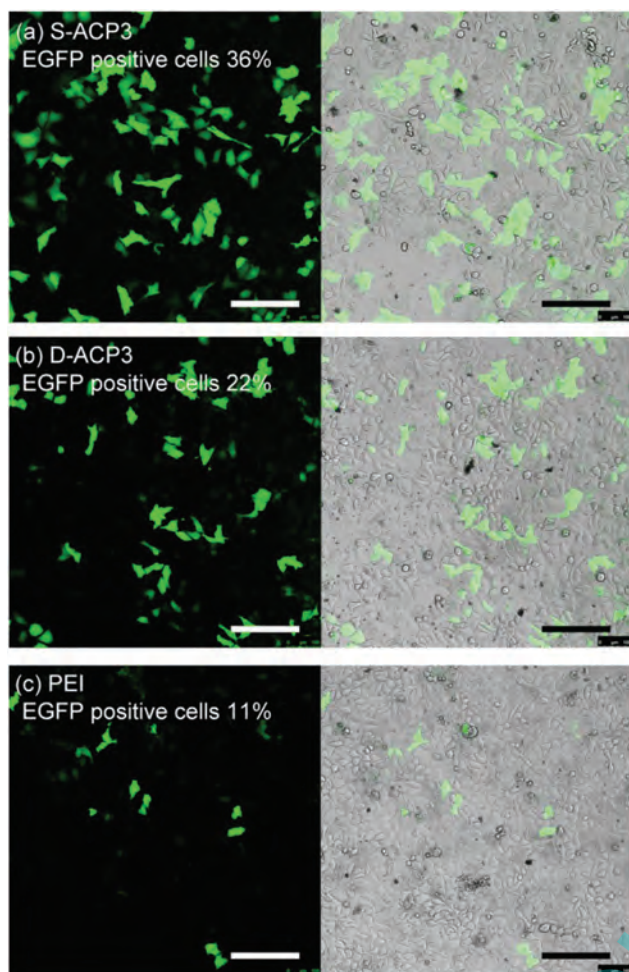
Fig. 7 Typical images of EGFP expression mediated by S-ACP3 (at its optimal N/P ratio of 25), D-ACP3 (at its optimal N/P ratio of 25), and PEI (at its optimal N/P ratio of 10) (scale bar = 200 μm).

hyperbranched structure could improve gene transfection performances, which might be due to the high density of positive charges of the supramolecular hyperbranched structure.[47]

Conclusions

In summary, we have successfully synthesized a series of PGMA-based cationic AB$_2$ macromonomers (Ad-(CD-PGEA)$_2$, ACP) *via* ATRP. ACPs could self-assemble into supramolecular hyperbranched polymers (S-ACP) due to the host–guest interaction between Ad and β-CD. S-ACP had better DNA condensation ability and transfection performances than its disassembled counterpart, demonstrating the positive effects of supramolecular hyperbranched topological structures on gene delivery. This kind of supramolecular hyperbranched polycation may provide a new concept to establish new gene delivery systems with low cytotoxicity and high transfection efficiency.

Notes and references

1 P. Sidaway, *Nat. Rev. Clin. Oncol.*, 2016, **13**, 64.
2 Y. Yue, I. M. Binalsheikh, S. B. Leach, T. L. Domeier and D. Duan, *Expert Opin. Orphan Drugs*, 2015, **3**, 1–15.
3 Y. Guo, W. Chen, W. Wang, J. Shen, R. Guo, F. Gong, S. Lin, D. Cheng, G. Chen and X. Shuai, *ACS Nano*, 2012, **6**, 10646–10657.
4 S. W. Lin and H. C. Ertl, *J. Future Virol.*, 2008, **3**, 491–503.
5 F. J. Xu and W. T. Yang, *Prog. Polym. Sci.*, 2011, **36**, 1099–1131.
6 J. Li, C. Yang, H. Li, X. Wang, S. H. Goh, J. L. Ding, D. Y. Wang and K. W. Leong, *Adv. Mater.*, 2006, **18**, 2969–2974.
7 J. R. Zhou, P. P. Chen, C. Deng, F. H. Meng, R. Cheng and Z. Y. Zhong, *Macromolecules*, 2013, **46**, 6723–6730.
8 X. Zheng, T. Zhang, X. Song, L. Zhang, C. Zhang, S. Jin, J. Xing and X. J. Liang, *J. Mater. Chem. B*, 2015, **3**, 4027–4035.
9 Q. L. Li, W. X. Gu, H. Gao and Y. W. Yang, *Chem. Commun.*, 2014, **50**, 13201–13215.
10 F. J. Xu, M. Y. Chai, W. B. Li, Y. Ping, G. P. Tang, W. T. Yang, J. Ma and F. S. Liu, *Biomacromolecules*, 2010, **11**, 1437–1442.
11 X. B. Dou, M. Y. Chai, Y. Zhu, W. T. Yang and F. J. Xu, *ACS Appl. Mater. Interfaces*, 2013, **5**, 3212–3218.
12 R. Q. Li, Y. Hu, B. R. Yu, N. N. Zhao and F. J. Xu, *Bioconjugate Chem.*, 2014, **25**, 155–164.
13 Y. Hu, Y. Zhu, W. T. Yang and F. J. Xu, *ACS Appl. Mater. Interfaces*, 2013, **5**, 703–712.
14 U. L. Rahbek, A. F. Nielsen, M. Dong, Y. You, A. Chauchereau, D. Oupicky, F. Besenbacher, J. Kjems and K. A. Howard, *J. Drug Targeting*, 2010, **18**, 812–820.
15 L. Wan, Y. Z. You, D. Oupicky and G. Z. Mao, *J. Phys. Chem. B*, 2009, **113**, 7.
16 D. Wang, T. Zhao, X. Zhu, D. Yan and W. Wang, *Chem. Soc. Rev.*, 2015, **44**, 4023–4071.
17 C. Tu, N. Li, L. Zhu, L. Zhou, Y. Su, P. Li and X. Zhu, *Polym. Chem.*, 2013, **4**, 393–401.
18 D. J. Chen, B. S. Majors, A. Zelikin and D. Putnam, *J. Controlled Release*, 2005, **103**, 273–283.

19 R. Dong, Y. Zhou, X. Huang, X. Zhu, Y. Lu and J. Shen, *Adv. Mater.*, 2015, **27**, 498–526.

20 X. H. Xu, Y. T. Jian, Y. K. Li, X. Zhang, Z. X. Tu and Z. W. Gu, *ACS Nano*, 2014, **8**, 9255–9264.

21 L. Yang, X. Tan, Z. Wang and X. Zhang, *Chem. Rev.*, 2015, **115**, 7196–7239.

22 X. Yan, F. Wang, B. Zheng and F. Huang, *Chem. Soc. Rev.*, 2012, **41**, 6042–6065.

23 R. Dong, Y. Zhou and X. Zhu, *Acc. Chem. Res.*, 2014, **47**, 2006–2016.

24 J. Hu and S. Liu, *Acc. Chem. Res.*, 2014, **47**, 2084–2095.

25 M. Paolino, H. Komber, L. Mennuni, G. Caselli, D. Appelhans, B. Voit and A. Cappelli, *Biomacromolecules*, 2014, **15**, 3985–3993.

26 F. Biedermann, U. Rauwald, J. M. Zayed and O. A. Scherman, *Chem. Sci.*, 2011, **2**, 279–286.

27 L. Yin, Z. Song, K. H. Kim, N. Zheng, N. P. Gabrielson and J. Cheng, *Adv. Mater.*, 2013, **25**, 3063–3070.

28 R. Dong, L. Zhou, J. Wu, C. Tu, Y. Su, B. Zhu, H. Gu, D. Yan and X. Zhu, *Chem. Commun.*, 2011, **47**, 5473–5475.

29 Q. L. Li, Y. Sun, Y. L. Sun, J. Wen, Y. Zhou, Q. M. Bing, L. D. Isaacs, Y. Jin, H. Gao and Y. W. Yang, *Chem. Mater.*, 2014, **26**, 6418–6431.

30 Q. D. Hu, G. P. Tang and P. K. Chu, *Acc. Chem. Res.*, 2014, **47**, 2017–2025.

31 G. Perez-Mitta, A. G. Albesa, W. Knoll, C. Trautmann, M. E. Toimil-Molares and O. Azzaroni, *Nanoscale*, 2015, **7**, 15594–15598.

32 P. E. Danjou, G. De Leener, D. Cornut, S. Moerkerke, S. Mameri, A. Lascaux, J. Wouters, A. Brugnara, B. Colasson, O. Reinaud and I. Jabin, *J. Org. Chem.*, 2015, **80**, 5084–5091.

33 B. Shi, K. Jie, Y. Zhou, J. Zhou, D. Xia and F. Huang, *J. Am. Chem. Soc.*, 2015, **138**, 80–83.

34 B. Yang, X. Dong, Q. Lei, R. Zhuo, J. Feng and X. Zhang, *ACS Appl. Mater. Interfaces*, 2015, **7**, 22084–22094.

35 Y. Shi, Z. Wang, X. Zhang, T. Xu, S. Ji, D. Ding, Z. Yang and L. Wang, *Chem. Commun.*, 2015, **51**, 15265–15267.

36 Q. L. Li, L. Wang, X. L. Qiu, Y. L. Sun, P. X. Wang, Y. Liu, F. Li, A. D. Qi, H. Gao and Y. W. Yang, *Polym. Chem.*, 2014, **5**, 3389–3395.

37 Y. Bai, X. D. Fan, H. Yao, Z. Yang, T. T. Liu, H. T. Zhang, W. B. Zhang and W. Tian, *J. Phys. Chem. B*, 2015, **119**, 11893–11899.

38 Y. Bai, X. D. Fan, W. Tian, T. T. Liu, H. Yao, Z. Yang, H. T. Zhang and W. B. Zhang, *Polym. Chem.*, 2015, **6**, 732–737.

39 H. Li, X. Fan, W. Tian, H. Zhang, W. Zhang and Z. Yang, *Chem. Commun.*, 2014, **50**, 14666–14669.

40 W. Tian, X. Fan, J. Kong, Y. Liu, T. Liu and Y. Huang, *Polymer*, 2010, **51**, 2556–2564.

41 R. Dong, Y. Su, S. Yu, Y. Zhou, Y. Lu and X. Zhu, *Chem. Commun.*, 2013, **49**, 9845–9847.

42 H. Zhang, X. Fan, R. Suo, H. Li, Z. Yang, W. Zhang, Y. Bai, H. Yao and W. Tian, *Chem. Commun.*, 2015, **51**, 15366–15369.

43 X. C. Yang, Y. L. Niu, N. N. Zhao, C. Mao and F. J. Xu, *Biomaterials*, 2014, **35**, 3873–3884.

44 S. Duan, X. Yang, F. Mei, Y. Tang, X. Li, Y. Shi, J. Mao, H. Zhang and Q. Cai, *J. Biomed. Mater. Res., Part A*, 2015, **103**, 1424–1435.

45 R. Dong, Y. Liu, Y. Zhou, D. Yan and X. Zhu, *Polym. Chem.*, 2011, **2**, 2771–2774.

46 H. Tian, J. Chen and X. Chen, *Small*, 2013, **9**, 2034–2044.

47 Q. F. Zhang, Q. Y. Yu, Y. Y. Geng, J. Zhang, W. X. Wu, G. Wang, Z. W. Gu and X. Q. Yu, *ACS Appl. Mater. Interfaces*, 2014, **6**, 15733–15742.